Cooling Performance: Exploring the Heat Mitigation Effect of Urban Trees with Computer Vision

Mikita Klimenka*, Simone Mora, Diaa Addeen Abuhani, Leslie Norford, Fábio Duarte*, Carlo Ratti

Senseable City Lab, Massachusetts Institute of Technology, 77 Massachusetts Avenue, Cambridge, 02139, Massachusetts, United States.

Contributing authors: klimenko@mit.edu; moras@mit.edu; diaa@mit.edu; lnorford@mit.edu; fduarte@mit.edu; ratti@mit.edu

*Corresponding author(s). E-mail(s): klimenko@mit.edu; fduarte@mit.edu

Abstract

Rising summer temperatures are placing increasing pressure on many cities to adapt public spaces for heightened heat stress. While the cooling benefits of urban trees are well documented, there remains a limited understanding of how these effects vary across tree types, morphologies, and urban contexts. This study addresses this knowledge gap by employing computer vision techniques to analyze thermal imagery of urban trees in four climatically diverse cities: Amsterdam, Boston, Dubai, and Los Angeles. Our findings reveal significant variation in cooling performance attributable to genera-specific traits, water consumption properties and surrounding environmental factors. By initiating a comparative analysis of urban tree types and their thermal performance, this research provides a foundation for more targeted and climate-responsive urban greening policies.

Keywords: Urban microclimate, urban vegetation, computer vision, urban cooling

1. Introduction

Global warming impacts the urban microclimate and leads to sudden, unexpected shifts in local temperatures that put communities at risk. During the 2003 European heatwave, almost 15,000 people across France died due to heat stress, primarily the elderly population in Paris, where temperatures rose above 45°C (De Bono et al.). Extreme heat events have since become regular in France, with similar episodes happening in 2019 and 2022, causing up to 11,000 deaths per year (Pascal et al.). Cities located in "temperate" or "mild" climate zones, such as Paris or Amsterdam, are now in dire need of identifying areas most vulnerable to heat waves and preparing their urban fabric accordingly.

Urban vegetation is known to have a cooling effect due to shading and evapotranspiration. The awareness of the cooling power of urban vegetation is centuries-old, with scrupulous studies documented in works like Luke Howard's 1818 "The Climate of London" (Howard et al.). Since then, the role of vegetation in mitigating urban heat has been extensively explored, and tree-planting schemes have been embraced at a policy level (Fu et al.). Despite the known positive impact of urban vegetation, there is a fragmented understanding of how the cooling power of urban trees varies across tree types, including shape, height, leaf area index (LAI) and other morphological properties of urban vegetation (Li et al.). This knowledge gap prevents cities from making efficient policy decisions on where and which trees they should plant. One example is the pervasive presence of palm trees in Los Angeles and Dubai. Despite the aesthetic appeal and historical signature, palms are not effective at shading or cooling, require higher maintenance, and are prone to issues like rodent infestation or fires (TreePeople).

Existing research on the cooling effects of urban trees is characterized by the diversity of complex methods and data sources (e.g. land surface temperature satellite data, thermal imagery, black globe measurements), as well as challenges in collecting data related to tree species and their morphology. Several studies explore street-level thermal imagery to examine the temperature of tree crowns (Irmak et al.) or look at the temperature of shade (Speak et al.). However, they rely on manual shade segmentation and thermal image processing which precludes these methods from scaling across geographic contexts.

In this paper, we explore morphology- and genera-specific cooling effects of trees leveraging thermal imagery and computer vision. We collected almost 2000 thermal and color image pairs along with environmental (air temperature and relative humidity) and tree genera data in Amsterdam, Boston, Dubai and Los Angeles, and measured canopies' surface temperatures and their relation to the surrounding urban surfaces. We examine how tree canopy temperature, shade temperature, and cooling of surrounding urban surfaces vary across tree genera, time of day, and tree morphology. We offer further discussion on how our methodology can be expanded to other contexts.

2. Results

Urban surface temperatures play a key role in influencing several physical variables relevant to the calculation of thermal comfort and heat balance (Voogt and Oke). We are primarily interested in the surface temperatures of three target regions that are impacted by the tree cooling effect: temperatures of tree crown, tree shade, and of the nearby urban surfaces adjacent to trees.

When comparing surface temperatures of target regions, we report our results as temperature delta. Surface temperature refers to the mean temperature as measured by a thermal camera. Temperature delta is the negative of the difference between the mean surface temperature of a target region (like a

tree canopy) and the mean surface temperature of nearby anthropogenic surfaces (building walls, road, pavement), which we refer to as the surrounding urban context. The objective of temperature delta is to compare how cooler or hotter a target region is relative to other surfaces within a single thermal image. This value accounts for effects that influence both surface types (e.g. shared shade or evening cooling) and estimate the tree's effect on surrounding surface temperatures relative to what they would have been without the tree in that location. Because we subtract tree temperature from the temperature of the context, which we expect to be higher, the temperature delta is typically a positive value, with higher value corresponding to a stronger cooling effect. Figure 1 explains the three target regions we chose. Further in this section, we explain in detail what types of surfaces we assign to the urban context to best describe the cooling effect of the target region.

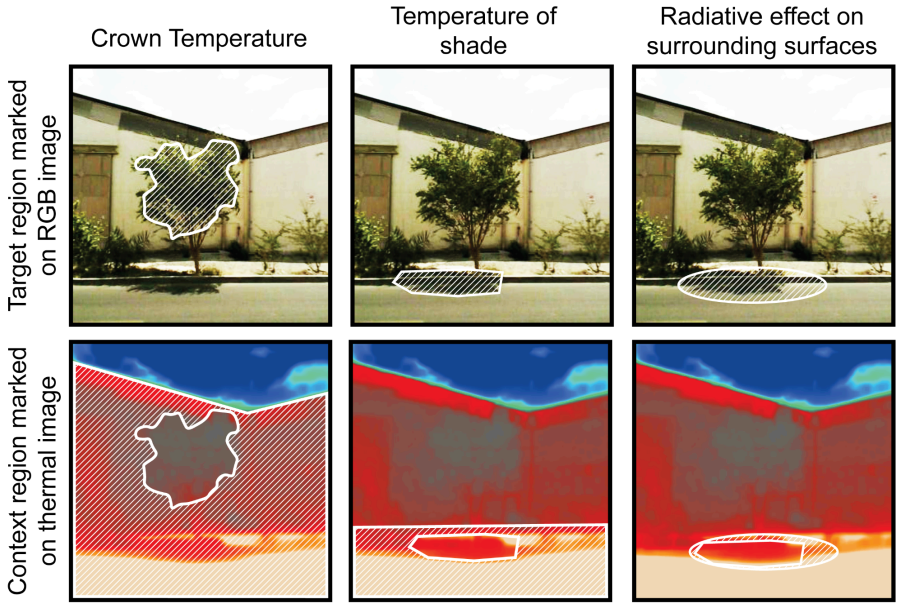

Figure 1: A diagram explaining our selection of the target region and the urban context, first detected in color photographs (first row) and calculated as mean values in the corresponding thermal images (second row).

Our data was collected in four cities - Los Angeles (February/March 2025), Dubai (March 2025), Amsterdam (June 2025) and Boston (June 2025). For each city, we collected almost 500 pairs of thermal and color images of trees, three times during the day. The supplementary material provides further details on specific tree locations and data collection times.

2.1 Tree Crown Temperature

In this section, the target region is the tree crown, and the temperature of the surrounding urban context is the mean temperature of all surfaces, excluding cars and the sky, after image segmentation (see Section 3: Methodology). We find that tree crowns are 2-10 °C cooler than the surrounding surfaces. We assume that in urban areas trees are more likely to occlude hotter buildings and other anthropogenic surfaces than the sky, which is colder in thermal images (Unsworth et al.). Below we explore how temperature deltas depend on the time of the day, orientation, morphology, and tree genera.

2.1.1 Heating of Canopy Crowns Throughout the Day

The temperature of urban surfaces rises from sunrise to noon as incident solar radiation increases, and falls as the sun sets. Through evapotranspiration, tree canopies can maintain their own temperature keeping it different from that of the surrounding urban surfaces.

Figure 2 demonstrates the change of temperature of tree crowns and the temperature of the urban context throughout the day for all four cities. Overall, the results show that trees maintain a cooler temperature than the surrounding urban surfaces by 2-15 ºC, depending on the context. During the morning shift, the temperature difference is the smallest, reaching as low as 2ºC in Los Angeles. Around noon, during peak solar hours, the difference is the largest, with trees being up to 10 ºC cooler than the surrounding surfaces (See Los Angeles data in Figure 2, at 1 PM). As the urban surfaces cool down later during the day, this difference eases to 4-5 ºC. When there is no incident radiation to power photosynthesis, the stomata close and evaporative cooling ends (Jackson et al.). In Los Angeles and Boston, we observe that by around 5 PM, the trees return to their original morning temperatures, while the urban surfaces are still hotter than they were in the morning.

Along with the field measurements from the handheld thermal camera, we report the ambient air temperature from a weather station (orange dots). In the presence of incident solar radiation, tree temperatures trail the air temperature (slightly above it), while anthropogenic surfaces heat up more due to lack of internal temperature regulation. It is worth noting that there is a light oscillating signal present in the anthropogenic and tree canopy measurements, which are arranged according to their timestamp. This is due to the changing orientation of trees and surfaces. As we traversed the neighborhoods, the direction of the photographs taken changed with the street grid, which was then reflected in the temperature changes. This also shows the lack of orientation bias throughout the session, where photographs from a specific direction did not get clustered in the beginning or the end of the session. Additionally, cloud cover and the diurnal solar path affect the difference in surface temperatures between trees and urban surfaces. In all cities except Amsterdam, both tree and urban surface temperatures remained above the ambient air temperature. This is due to a significant absorption of solar radiation under sunlight. In Amsterdam, conversely, surface temperatures were lower due to heavy cloud cover filtering direct radiation.

Note that there are some slight differences between the data collection methods. In Amsterdam, Dubai, and Boston, each tree was scanned three times during the corresponding morning, afternoon, and evening traverses, while in Los Angeles, we moved continuously throughout the city. In Boston and Los Angeles, all 500 images were collected in one day, while in Dubai and Amsterdam, only part of the total 500 images collected is reported. The Methodology section provides further clarification of these differences.

In Dubai, the increase and decrease of temperature of urban surfaces throughout the measurement period is not as prominent as in the other three cities, even though it generally tends to be lower earlier in the morning. We attribute this phenomenon to higher temperatures and longer light hours in Dubai: the heating of the surfaces begins earlier in the day, and the subsequent cooling happens later. This is consistent with the data captured in the other traverses. Unlike Los Angeles, trees in Dubai maintain a temperature that is closer to the ambient air temperature. This may be due to several reasons: 1) the use of local temperature measurements in Dubai against a centralized weather station in Los Angeles; 2) different tree genera, climate type, and dynamics due to season; and 3) the fact that Dubai measurements were conducted under a much higher ambient temperature.

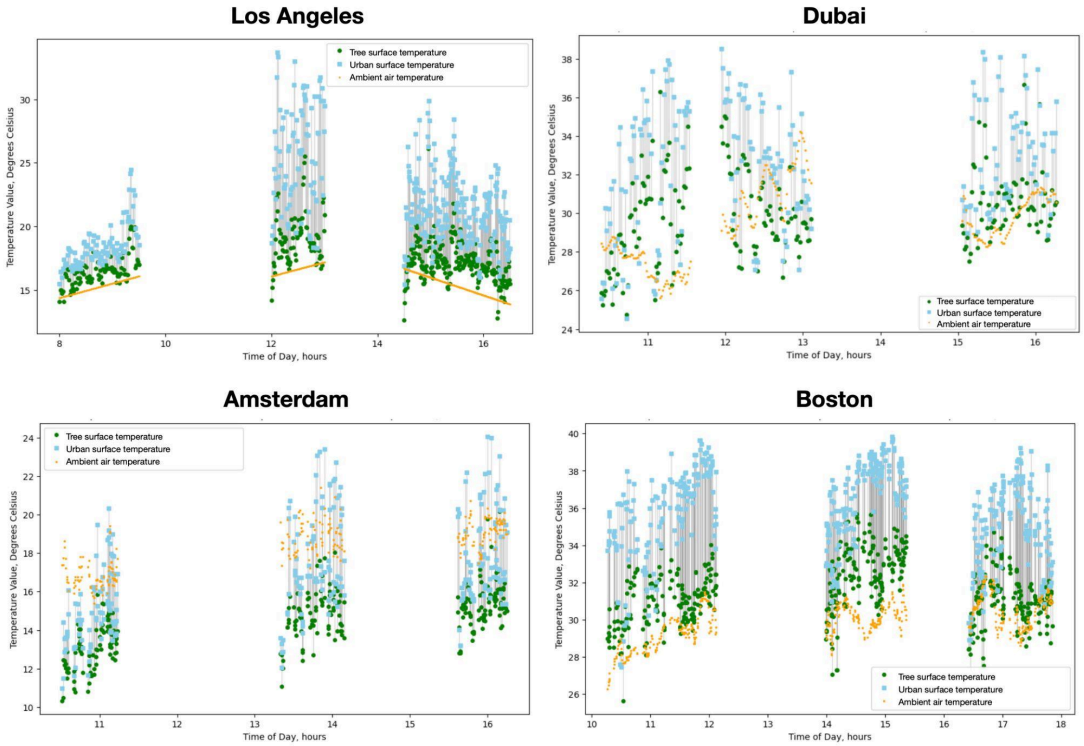

Figure 2 : Change of temperature of tree crowns and the temperature of the urban context throughout the day, reported across four cities. The data for Dubai in Figure 2 is reported for one of three different neighborhoods (Gardens), because the collection was split between three neighborhoods. The data for Amsterdam is reported for one of the two traverses (on May 26th)

2.1.2 Impact of Tree Genera on the Difference in Canopy Crown Temperature

We hypothesize that the diurnal variations of tree crown temperatures and their corresponding canopy deltas differ due to tree canopy structure, leaf shape, density, patterns of evapotranspiration, and overall health. Practitioners are not able to tune each of these parameters individually, as they vary greatly depending on tree types. Therefore, we examine how the choice of tree genera affects these parameters comprehensively. The distribution of tree genera in cities is long-tailed. Therefore, we report the results for several most commonly occurring genera in a given city. The number of genera chosen per city and classification is further explained in the Methods section.

Figure 3 shows crown temperature deltas as barplots for different tree genera, reported for all four cities. We find that, in general, the variation of temperatures within a given genus is larger than variation between different genera, with several exceptions. For example, ulmus in Amsterdam and Boston has higher temperature delta, while in Dubai, Azadirachta (which includes predominantly Neem trees in our dataset) has a slightly higher delta, meaning that it has a stronger cooling effect.

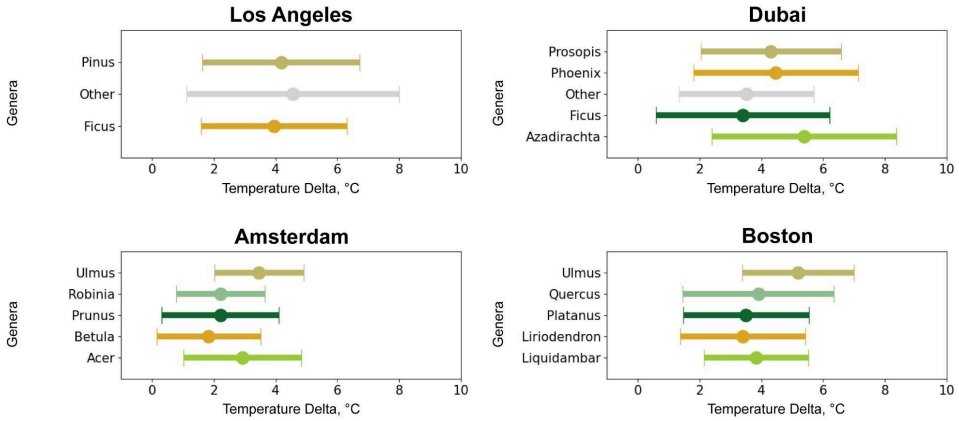

Figure 3: Tree crown temperature deltas across tree genera and four cities

2.1.3 Other effects - morphology and orientation

In the supplementary section, we report the impacts of orientation on the temperature of tree crowns (Figures A2 and A3 with experiments performed in Dubai and Los Angeles only). The effect of orientation at different times of the day is self-explanatory: areas facing the sun (such as south side at noon or west side in the afternoon) heat up more due to more sun exposure. We found no significant effects of tree width, cross-section area, or height on canopy temperature.

2.2 Temperature in the Tree Shade

In this section, our target region is the urban surface that is located in the shade of a tree. Shade delta refers to the difference in temperature between an urban surface in tree shade and outside of it. We studied shade deltas by three types of urban surfaces: building wall, asphalt, and grass. We report this comparison across three cities (Boston, Dubai, Los Angeles). Due to overcast sky conditions of Amsterdam, too few images had explicit shadows, which is why we excluded it from this comparison.

Figure 4 reports the results. If an insufficient number of images were collected for a specific genus in the context of a particular urban surface, the data for it was omitted. Overall, shade deltas do not show variation between genera. The difference between shade delta on building wall, asphalt, and grass surfaces is worth noting when considering the juxtaposition of tree cooling and effects of urban geometry. Across Boston, Dubai, and Los Angeles, shade delta associated with building wall surfaces tends to be lower due to the shorter time a shadow is cast onto a vertical surface. In Los Angeles, grass surface deltas are around 0 °C, while the asphalt surface deltas are around 3 °C. In Dubai, the grass delta is around 4.5 °C and the asphalt delta is around 5 °C. In Boston, the grass delta is around 1 °C and the asphalt delta is around 3 °C. This is unsurprising since grass surfaces, like other types of vegetation, are cooler than asphalt. As a result, the effect of tree shadow is partially offset by the evapotranspiration effects that cool grass, and shading anthropogenic surfaces leads to greater reduction of overall urban surface temperatures.

During our experiment in Los Angeles in February, the air temperature was relatively low and the sky was overcast during most of the day. We believe that the total incident solar radiation was not sufficient to heat up grass surfaces enough to maintain a different temperature from the grass surfaces in shade, hence the grass surface delta is around 0 °C.

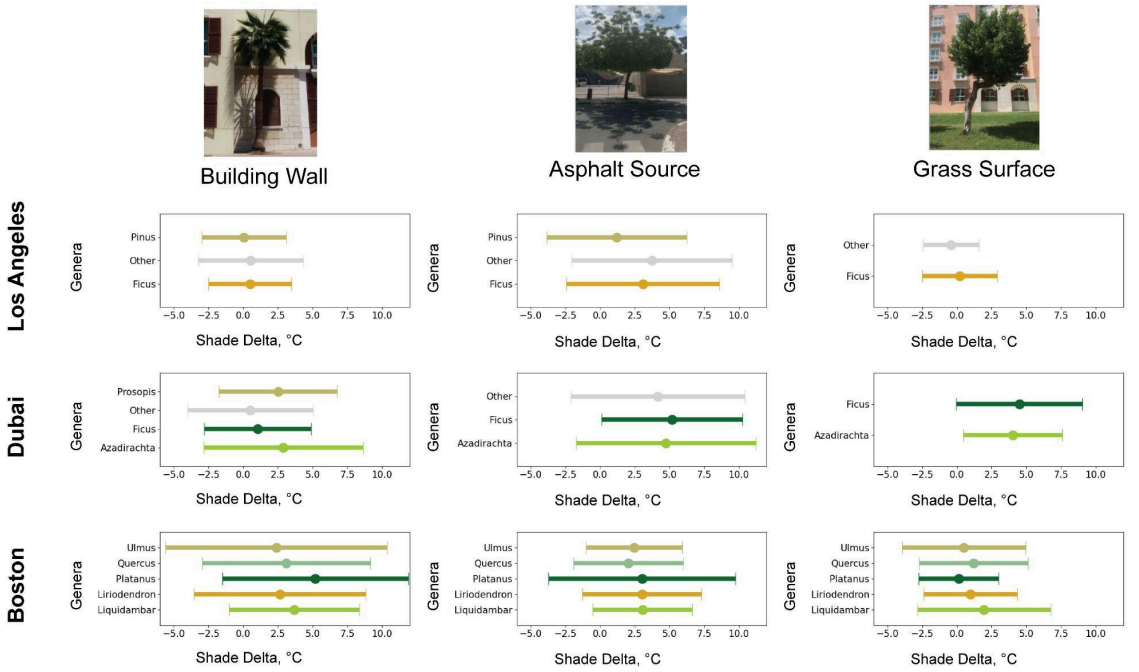

Figure 4: Shade deltas cast on three types of urban surfaces, reported across three cities.

2.3 Radiative Effect of Trees on Urban Surfaces

In this section, our target region is an area directly under the tree as described in Figure 1. We hypothesize that there may be minor effects of mutual radiative exchange between trees and close anthropogenic surfaces that lead to the cooling of the latter. Here we also include the effect of shadows that had been incident on a surface close to the tree during the day but had moved during the time of thermal capture. To better capture this effect, we exclude areas in tree shade by applying the negative of the shade mask. Examples of those are seen in Figure A1 in the supplementary information. Figure 5 reports these results by cities. Due to the weak nature of these effects, the temperature deltas are generally lower than they are for shadows. Most mean values are around 0 °C, and the deltas have high spread both in the positive and negative temperature range. Overall, such radiative effects do not significantly contribute to urban heat reduction. We attribute this to the fact that such radiative effects may only be visible upon very close thermal scanning of trees.

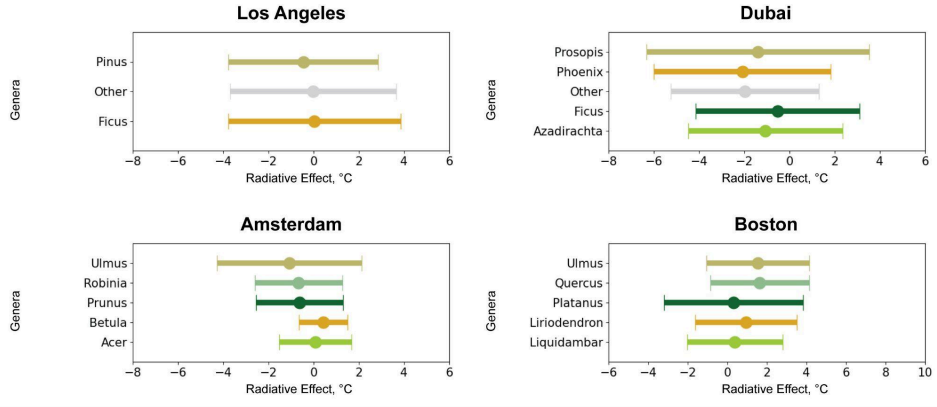

Figure 5: Radiative effect by tree genera in the four cities.

2.4 Tree Cooling Efficiency

So far we have considered trees solely as subjects that exist outside of the human-made infrastructure and provide the virtue of cooling solely at nature's grace. But it is also important to highlight what kind of resources trees consume, how these resources put a price tag to their cooling effects, and how this tradeoff affects urban planting strategies.

Transpiration requires a tree to absorb water from the soil. In dense urban areas soils are not necessarily connected well to natural aquifers, while the density of trees within a city may be higher than in the surrounding biomes, particularly in Dubai and Los Angeles, and to a smaller extent in Amsterdam. Trees require consistent and extensive irrigation, which also implies economic and environmental costs associated with water transportation and retrieval. For example, does the energy cost and environmental footprint of transporting water to a park in Dubai justify planting more trees or trees of different types, or could these efforts be diverted to simpler methods for urban cooling, such as shaders or misters? While the benefits of trees extend beyond urban heat mitigation to biophilic effects (Lefosse et al.) and air quality improvement(Nowak et al.), quantifying their cooling efficiency is important for cities when planning urban green infrastructure.

Equation 1 below describes our definition of tree cooling efficiency metric. If a tree is considered as a device that maintains a certain canopy temperature delta **dT** and has a canopy cross-section area facing the pedestrian as ***A***, then it is responsible for ***dT * A*** 'heat flux'. The cost for generating this thermal flux can be represented as the amount of water consumed. Location-specific water consumption data for tree genera is sparse, with values reported in a wide range of ways, from mean values per tree to metrics that account for tree height and canopy area. We express the volume of water consumed by trees daily as ***C*h*** where ***h*** is the height of irrigation (similar to precipitation height), and ***C*** is catchment area, that is the area of the soil reached by tree roots, where the incident water is absorbed. Representing tree cooling efficiency as the amount of reduced radiative flux per liter of water consumed per day for a specific tree can allow cities to link these metrics further to the energy costs of desalination and water delivery,depending on the economic context of urban water supply. We note that the catchment area ***C*** and canopy cross-section ***A*** both increase with tree size and may thus be linearly related. We therefore may simplify the equation as:

$$Tree\ Cooling\ Efficiency\ = \frac{MRT\ flux\ reduction}{Water\ Consumption\ Cost} = \frac{A * dT}{C * h} \Leftrightarrow \frac{dT}{h} \quad (1)$$

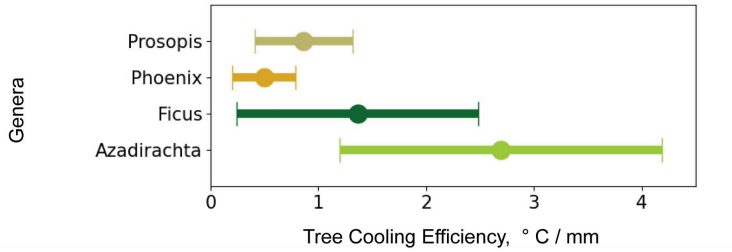

Figure 6: Comparison of tree cooling efficiencies with respect to water consumption in Dubai. Neem, a native genera, is a clear winner, while palm trees are least efficient. Note that the differences are much more significant than what we observe when only the cooling effect is considered without considerations of water consumption.

Table 2 in the Supplementary Information describes in detail the process of assigning tree water consumption data for different genera. Figure 6 describes the calculated cooling efficiency metrics of different genera. In Dubai, it is evident that palm trees are significantly less efficient than other genera due to the high water consumption rates. Overall, we find that the variations in water consumption

ranges significantly more than the overall cooling effects due to tree canopy temperatures that we found, which means that irrigation cost is a defining factor in the cooling effect of urban vegetation.

Equation 1 is a significant simplification of the trade-off between water consumption and cooling effect. The water consumption of trees depends on many granular factors, such as height, canopy shape, age, health, and soil conditions. Detailed research on these factors for specific genera is scarce and is limited to narrow case studies. In the absence of such detailed comparisons, we assumed average genus-specific water consumption rates given the similarity of trees planted in a particular urban area. Urban visual data, however, allows the extraction of other properties of trees such as height, canopy shape, and even health conditions and may allow urban researchers to compute tree-specific cooling efficiency provided that water consumption rates are known.

3. Discussion

We have measured that trees maintain a significantly lower temperature than other urban surfaces and tend to trail air temperature values closely. Based on our exploration of tree cooling effects in Amsterdam, Boston, Dubai, and Los Angeles, we have established time of day (along with incident solar radiation and air temperature) to be important factors shaping the thermal signature of urban trees. We have introduced a method to assess the cooling efficiency of trees as a trade-off between their water consumption costs and the reduction of overall urban surface temperatures. While most tree genera retain similar temperature deltas in cities (with some exceptions like ulmus in Amsterdam or neem in Boston), differences in their water consumption rates play a key role in determining their overall efficiency. This is particularly evident for certain genera like palm trees that consume significantly more water than other genera while providing similar or smaller cooling effects. Using the tools of thermal imagery and computer vision, we laid the foundation for a scalable approach to studying trees' cooling powers in urban contexts. We have shown how tree cooling efficiency can be measured in three distinct ways: cooling related to crown temperatures, temperature of shadows, and near-tree radiative effects. We envision this approach to be used by cities to further study factors affecting tree cooling efficiency on a more granular scale. Below we list some other avenues for future exploration.

Sky conditions
We expect a lower temperature difference between tree crowns and the surroundings under overcast skies, which we cannot precisely quantify without measurements of global and diffuse radiation. Cloud cover also affects the ambient temperature and the overall amount of solar radiation incident on urban surfaces including trees.

Humidity
The saturation of air with water has a strong effect on the rates of evaporation, which in turn defines the extent to which a tree cools itself.

Performance of tree Genera Across Biomes
The extent to which different trees adapt and thermally perform in other cities depends on local climate, irrigation levels, pressure, humidity, and soil quality.

Irrigation Rates
When estimating the cooling efficiency of trees of different genera, we have assumed that they were irrigated at the exact rate required. Some sources suggest (Al Yamani et al.) that trees indeed consume the amount of water they require, which motivates urban planners to calculate those minimum rates with some safety factor. Further work is required to account for these differences.

4. Methods

4.1 Site Selection and Time

Our choice of cities was influenced by research availability and diversity of climate and geography. Table 1 below summarizes collection times and Köppen climate classifications.

Table 1. Data Collection times and climate classification, by city

City	Köppen Classification (Peel et al.)	Data Collection times
Los Angeles	Csa (Hot-summer Mediterranean)	February 28 - March 2, 2025
Dubai	BWh (Hot desert)	March 19 - 21, 2025
Boston	Dfa (Hot-summer Humid continental)	June 12, 2025
Amsterdam	Cfb (Oceanic)	May 23, May 26, 2025

4.2 Data Collection

Several modes of data collection were attempted, including mounting a custom-made 360-degree camera on a vehicle, recording from a commercial phone-based thermal camera from a moving vehicle, biking, and taking handheld photographs. Taking handheld photographs with a commercial thermal camera was found to be the most convenient way to obtain clear, unobstructed images. The exposure time prevented taking images from a moving vehicle and required taking thermal images statically. For data collected in Boston, Dubai, and Los Angeles, we used a commercial FLIR One Edge Pro[1] camera (c.ca 500USD) mounted on a smartphone and walked along streets in target cities to capture photographs of trees. For Amsterdam only, we used FLIR One Pro. Due to the dense planting of trees in pre-defined neighborhoods, we were able to quickly switch between multiple trees, at a rate of circa 60 trees per hour. A sample of the datapoint is displayed in Figure 7. The process of data collection and equipment is captured in Figure 8.

Thermal images, recorded in grayscale, were uploaded to the camera's cloud service (FLIR Ignite), where they were downloaded in bulk along with color images. We used the FLIR Studio to export color-gradient bars that mapped single-channel pixel values to a color range from 0 to 40 ºC. We subsequently used these bars to convert thermal images into a linear temperature scale and map temperature values for each pixel value. We used tools provided by the camera manufacturer to prepare color maps and temperature gradients for data visualization, including Figures in this manuscript, while grayscale originals were used for analysis. At the time of image capture, the camera thermal range was manually set to 0-40 degrees Celsius. This decision was made for convenience of visualization and processing as we expected most of our recorded temperatures to fall in the range of 10-40 degrees Celsius. An additional decrease to 0 degrees was made to accommodate a clear separation of sky that typically is recorded below 0 ºC by thermal cameras.

To record ambient temperature and pressure, we used a Kestrel 5400 Heat Stress Tracker. Normally, this device is primarily used for estimating MRT and outdoor thermal comfort as it features a black globe. In our experiment, however, we used it to record ambient temperature and relative humidity. The Kestrel worked paired with its smartphone app for data storage. Because the FLIR camera was using the phone's bluetooth and WiFi signal, a second smartphone was used to run the Kestrel App. In addition to the Kestrel App, the GPS Camera App was used to record the orientation, timestamp and

[1] FLIR Systems. *FLIR ONE Edge Pro.* Teledyne FLIR, https://www.flir.com/products/flir-one-edge-pro/. Accessed 10 Apr. 2025

geo-location of the photographs. Since the app required taking a photograph, we also kept a high-resolution dataset of tree images that we used for classification and alignment checks. Figure 8 summarizes the devices and corresponding apps used to collect the data.

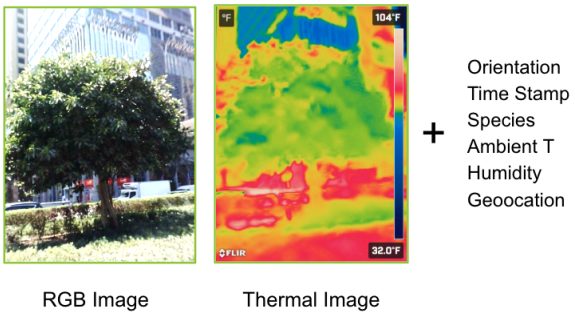

Figure 7: Sample datapoint collected that includes a color image, a thermal image, and metadata.

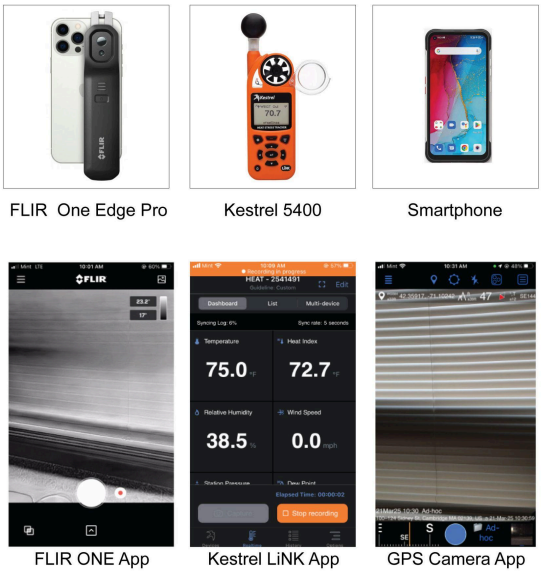

Figure 8: Overview of devices used with corresponding smartphone apps

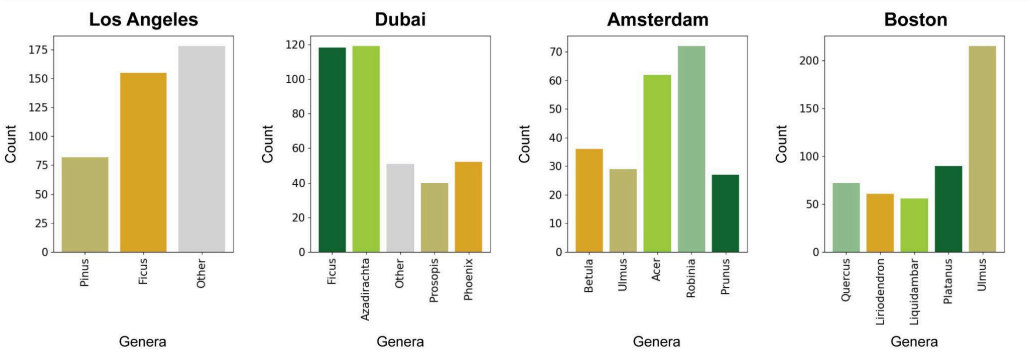

Figure 9: Total number of images collected by genera

4.3 Image Processing

Because detecting tree canopies is a common task in computer vision, we resorted to using a ResNet-50 trained on the ADE20K dataset.[2] To adapt the model to sparse crowns where sky or the building wall shows behind, we additionally applied a green pixel mask, selecting values with < 60 value in the green channel. After the tree mask was detected, we applied it to the thermal image and calculated the mean of all temperature pixels within the tree mask.

To build our dataset, we picked trees that clearly stood against a wall or a building and were not in a cluttered scene. Additionally, we did not select trees that visibly had no leaves or very sparse canopies so that we can count on the segmentation network picking up only the pixels in the canopy. If the project is to be scaled up to more complex urban settings where trees occlude each other, e.g. parks, tree canopy masking may quickly become a challenge.

Additionally, we calculated the mean temperature of other urban surfaces. To do so, we computed the mean of all temperature pixels outside of the tree mask. Additionally, we removed the pixels that were segmented as sky or cars. The sky is not an urban surface and is much cooler than any urban materials. Cars are mobile urban elements, not permanent surfaces. Even though they contribute to urban heat significantly, their presence might bias the images that do not have cars and significantly skew the temperature of the urban surfaces. Other potentially disrupting objects like people were not captured at large in the dataset. We used these two values to calculate what we refer to as canopy delta—the difference between the mean temperature of the tree crown and the mean temperature of all other urban surfaces. Figure 10 summarizes the process.

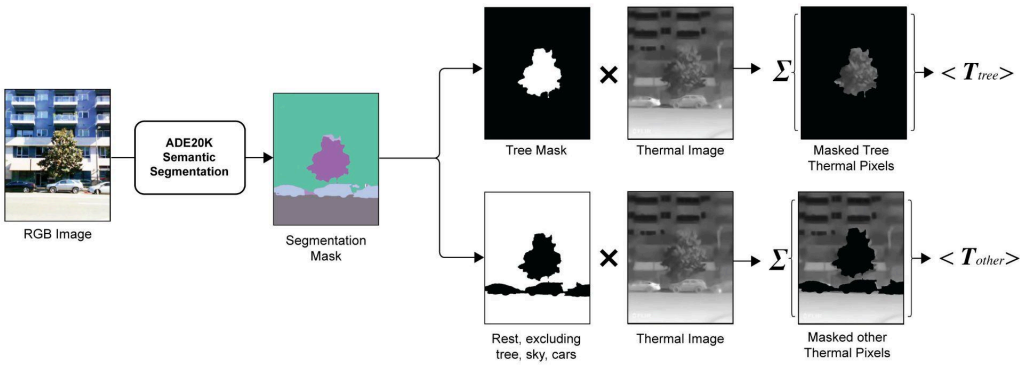

Figure 10: Segmentation of tree canopies

Segmentation of tree shadows

The process of segmenting tree shadows was similar to tree canopies. However, because shadow is not a part of the labels within the ADE20K dataset, we resorted to using a foundational model CLIPSeg (Lüddecke and Ecker). Prompt 'shadow' was passed to the CLIP-based model that identified an attention mask most associated with the semantic encoding of the word in the picture. The attention mask was later thresholded, and the largest thresholded segment was chosen (if there were several non-contiguous regions within the image) (See Figure 11). Although it is not shown in the diagram, pixels of certain darkness (where all three channels are below 50) were masked out as well to prevent comparison with other shaded regions. Subsequently, the shadow mask was overlapped with the ADE20K-based segmentation mask of the non-tree region (buildings, walls,

[2] CSAILVision. *semantic-segmentation-pytorch*. GitHub, https://github.com/CSAILVision/semantic-segmentation-pytorch. Accessed 10 Apr. 2025.

grass, sidewalk, road), and the mean temperature within the region was computed to return the temperature in the shadow. Similarly, the temperature outside the shadow was calculated. In order to compare against different urban materials (building walls, asphalt, grass), we modified the Semantic Mask to be limited to one of these categories.

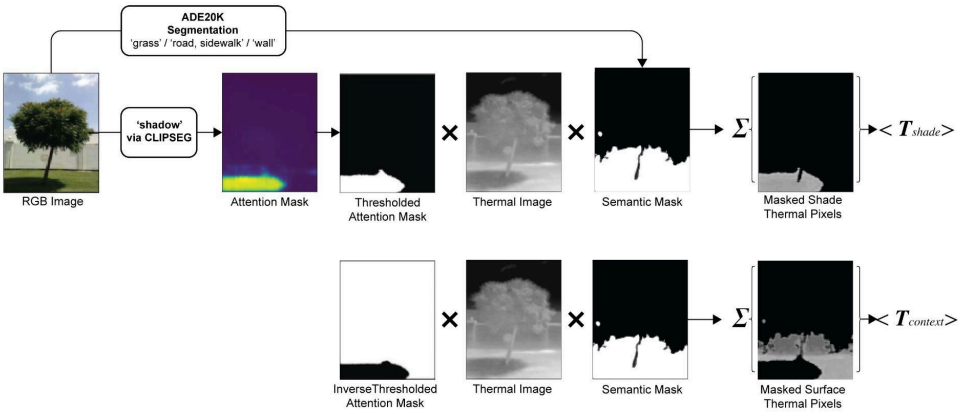

Figure 11: Segmentation of tree shadows

Segmentation of areas under the tree for radiative studies

Leveraging previous methods of shadow and tree detection, we obtained a sampling area under the tree for radiative studies as explained in Figure 12. First, we used a bounding box for trees obtained with Yolo trained on Objects365 (Glenn et al.) and identified the lower boundary of the box. We subsequently traced an elliptical area with the vertical radius of 25% of the height of the bounding box. Using the masks for shadows, we excluded shadows from the sampling area. The remaining area was assigned to either ‘grass’ or ‘asphalt’ depending on the segmentation mask of the urban scene. These areas were used to sample mean temperature due to radiative exchange.

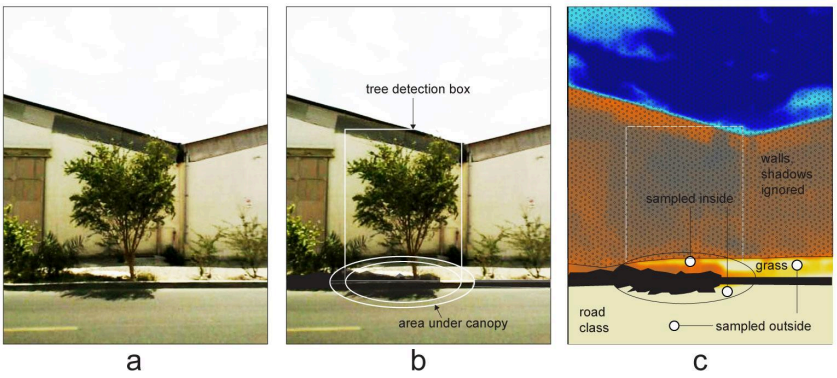

Figure 12: Isolation of the sampling region around the three for the study of irradiation exchange. a) original color image b) detection box along with the area under the canopy c) segmentation of the shadows (tree and context) and sampling of corresponding materials (road and grass) under the canopy and outside in the rest of the image.

5. Supplementary Information

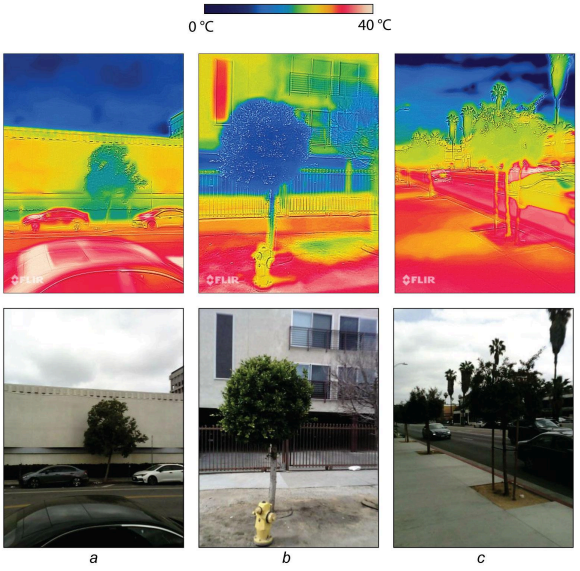

Figure A1: Examples of cases where there is a cooling effect of an area next to the tree without an apparent presence of a clear shadow in the color photograph. a) The cooling of a wall due to a combination of shading and irradiation in diffused sunlight. b) The shadow is present but is very faint. There is a clear gradient of shadow cooling, due to variation in canopy density as well as due to shadow mobility c) the presence of a cooling of the pavement in three directions from the tree without an apparent shadow. This was captured in diffuse sunlight after the sky became cloudy. We hypothesize that there was a shadow cast previously to the left of the tree which disappeared, leaving an apparent cooling effect.

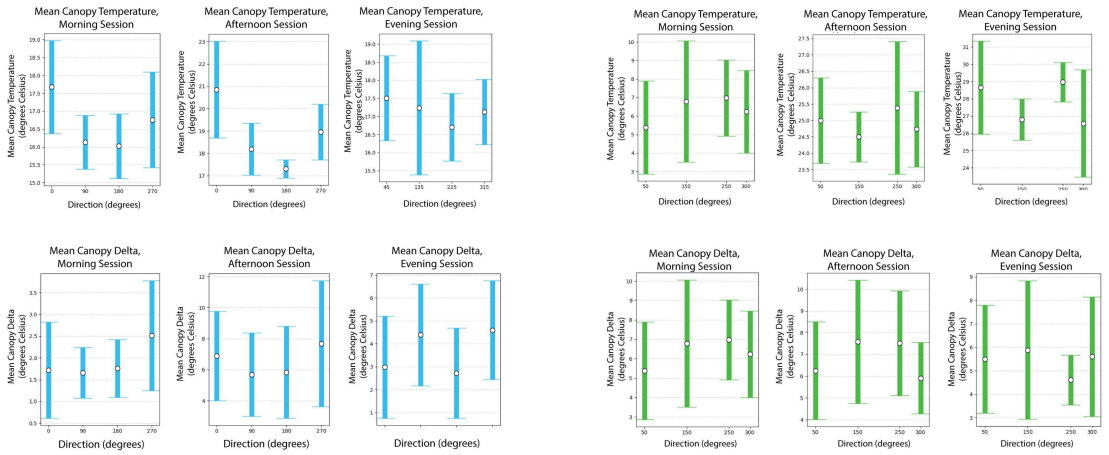

Figure A2: Bar plots demonstrating the impact of direction on crown temperatures and temperature deltas in (1) Los Angeles and (2) Dubai

Table 2: Water Consumption Rates of Different Tree Genera L/day

Genus	**Water Consumption Rate, L / day**	**Water Consumption Rate *h*, mm / day**
Dubai		
Phoenix	324([3])	9.0
Prosopis	180 ([4])	5.0
Azadirachta	72 ([5])	2.0
Ficus	90 ([6])	2.5

[3] Kassem, M. A. "Water requirements and crop coefficient of date palm trees Sukariah CV." *Misr Journal of Agricultural Engineering* 24.2 (2007): 339-359. The authors report irrigation between 4 and 14 mm for a 36 sq.m. irrigation area per day, which amounts to 324 l/day if an average is taken (9 mm)

[4] Taken from irrigation requirements in April from Table 1: Al Yamani, Wafa, et al. "Water use of Al Ghaf (Prosopis cineraria) and Al Sidr (Ziziphus spina-christi) forests irrigated with saline groundwater in the hyper-arid deserts of Abu Dhabi." *Agricultural Water Management* 203 (2018): 105-114. Although the authors report 35 L/day in April, they also reference 5 mm / day. Given that we want to compare plants on the same scale, we use this value with palm's catchment area of 36 sq.m. to obtain

[5] Meena, Vijay Singh. "What Are the Annual Water Requirements of the Neem Plant in an Arid Climate?" *ResearchGate*, 12 May 2015. The author states that 400-1200 mm of annual rainfall is sufficient. Taking 800 mm as a median value, and assuming the same catchment area as for palm (36 sq.m), we obtain 2mm per day for 36 sq.m, which is 72 L / day

[6] Tapia, R., et al. "Effect of four irrigation rates on growth of six fig tree varieties." *II International Symposium on Fig 605*. 2001. The authors reference 900 mm of irrigation, which we assume to be 2.5 mm/day. Taking the same catchment area as for a palm, we obtain 90 L / day.

Bibliography

1. De Bono, Andrea, et al. *Impacts of Summer 2003 Heat Wave in Europe*. United Nations Environment Programme, Mar. 2004, https://www.unisdr.org/files/1145_ewheatwave.en.pdf.

2. Pascal, Mathilde, et al. "A Yearly Measure of Heat-Related Deaths in France, 2014–2023." *Discover Public Health*, vol. 21, no. 44, 2024, https://link.springer.com/article/10.1186/s12982-024-00164-3.

3. Howard, Luke. *The climate of London*. Vol. 2. W. Phillips, sold also by J. and A. Arch, 1818.

4. Fu, Jiawei, et al. "Optimized greenery configuration to mitigate urban heat: A decade systematic review." *Frontiers of Architectural Research* 11.3 (2022): 466-491.

5. Li, Haiwei, et al. "Cooling efficacy of trees across cities is determined by background climate, urban morphology, and tree trait." *Communications Earth & Environment* 5.1 (2024): 1-14.

6. TreePeople. (2017, November 14). *A future without palm trees in LA*. TreePeople. https://treepeople.org/2017/11/14/palm-death/

7. Irmak, Mehmet Akif, et al. "Assessment of the effects of different tree species on urban microclimate." *Environmental Science and Pollution Research* 25 (2018): 15802-15822.

8. Speak, Andrew, et al. "The influence of tree traits on urban ground surface shade cooling." *Landscape and urban planning* 197 (2020): 103748.

9. Voogt, James A., and Timithy R. Oke. "Complete urban surface temperatures." *Journal of applied meteorology* 36.9 (1997): 1117-1132.

10. Unsworth, Michael H., and J. L. Monteith. "Long‐wave radiation at the ground I. Angular distribution of incoming radiation." *Quarterly Journal of the Royal Meteorological Society* 101.427 (1975): 13-24

11. Jackson, R. D., et al. "Estimation of daily evapotranspiration from one time-of-day measurements." *Agricultural Water Management* 7.1-3 (1983): 351-362.

12. Lefosse, D. C., Duarte, F., Sanatani, R. P., Kang, Y., van Timmeren, A., Ratti, C. (2025). Feeling Nature: Measuring perceptions of biophilia across global biomes using visual AI. npj Urban Sustainability

13. Nowak, David J. "The effects of urban trees on air quality." *USDA forest service* 96 (2002): 130413867.

14. Al Yamani, Wafa, et al. "Water use of Al Ghaf (Prosopis cineraria) and Al Sidr (Ziziphus spina-christi) forests irrigated with saline groundwater in the hyper-arid deserts of Abu Dhabi." *Agricultural Water Management* 203 (2018): 105-114.

15. Peel, M. C., B. L. Finlayson, and T. A. McMahon. "Updated world map of the Köppen–Geiger climate classification." *Hydrology and Earth System Sciences*, vol. 11, no. 5, 2007, pp. 1633–1644.

16. CSAILVision. *semantic-segmentation-pytorch*. GitHub, https://github.com/CSAILVision/semantic-segmentation-pytorch. Accessed 10 Apr. 2025.

17. Lüddecke, Timo, and Alexander Ecker. "Image segmentation using text and image prompts." *Proceedings of the IEEE/CVF conference on computer vision and pattern recognition*. 2022

18. Glenn Jocher, et al. *YOLOv5 by Ultralytics*. GitHub repository, 2020. Dataset: **Objects365** – Shiyang Li, Zeming Li, Runhui Huang, Guan Huang, et al. *Objects365: A Large-scale, High-quality Dataset for Object Detection*. ICCV 2019.

19. Kassem, M. A. "Water requirements and crop coefficient of date palm trees Sukariah CV." *Misr Journal of Agricultural Engineering* 24.2 (2007): 339-359.

20. Taken from irrigation requirements in April from Table 1: Al Yamani, Wafa, et al. "Water use of Al Ghaf (Prosopis cineraria) and Al Sidr (Ziziphus spina-christi) forests irrigated with saline groundwater in the hyper-arid deserts of Abu Dhabi." *Agricultural Water Management* 203 (2018): 105-114.

21. Meena, Vijay Singh. "What Are the Annual Water Requirements of the Neem Plant in an Arid Climate?" *ResearchGate*, 12 May 2015, www.researchgate.net/post/What-are-the-annual-water-requirements-of-the-Neem-plant-in-an-arid-climate

22. Tapia, R., et al. "Effect of four irrigation rates on growth of six fig tree varieties." *II International Symposium on Fig 605*. 2001